

NRC Publications Archive Archives des publications du CNRC

Higher-order structure of human chromosomes observed by electron diffraction and electron tomography

Hayashida, Misa; Phengchat, Rinyaporn; Malac, Marek; Harada, Ken; Akashi, Tetsuya; Ohmido, Nobuko; Fukui, Kiichi

This publication could be one of several versions: author's original, accepted manuscript or the publisher's version. / La version de cette publication peut être l'une des suivantes : la version prépublication de l'auteur, la version acceptée du manuscrit ou la version de l'éditeur.

For the publisher's version, please access the DOI link below. / Pour consulter la version de l'éditeur, utilisez le lien DOI ci-dessous.

Publisher's version / Version de l'éditeur:

<https://doi.org/10.1017/S1431927620024666>

Microscopy and Microanalysis, 27, 1, pp. 149-155, 2020-11-20

NRC Publications Archive Record / Notice des Archives des publications du CNRC :

<https://nrc-publications.canada.ca/eng/view/object/?id=5d07835b-749b-471c-b003-3130393832e6>

<https://publications-cnrc.canada.ca/fra/voir/objet/?id=5d07835b-749b-471c-b003-3130393832e6>

Access and use of this website and the material on it are subject to the Terms and Conditions set forth at

<https://nrc-publications.canada.ca/eng/copyright>

READ THESE TERMS AND CONDITIONS CAREFULLY BEFORE USING THIS WEBSITE.

L'accès à ce site Web et l'utilisation de son contenu sont assujettis aux conditions présentées dans le site

<https://publications-cnrc.canada.ca/fra/droits>

LISEZ CES CONDITIONS ATTENTIVEMENT AVANT D'UTILISER CE SITE WEB.

Questions? Contact the NRC Publications Archive team at

PublicationsArchive-ArchivesPublications@nrc-cnrc.gc.ca. If you wish to email the authors directly, please see the first page of the publication for their contact information.

Vous avez des questions? Nous pouvons vous aider. Pour communiquer directement avec un auteur, consultez la première page de la revue dans laquelle son article a été publié afin de trouver ses coordonnées. Si vous n'arrivez pas à les repérer, communiquez avec nous à PublicationsArchive-ArchivesPublications@nrc-cnrc.gc.ca.

MICROSCOPY AND MICROANALYSIS



The higher-order structure of human chromosomes observed by electron diffraction and electron tomography

Journal:	<i>Microscopy and Microanalysis</i>
Manuscript ID	MAM-20-X-176.R2
Manuscript Type:	Original Article
Date Submitted by the Author:	n/a
Complete List of Authors:	Hayashida, Misa; NRC; Phengchat, Rinyaporn; Kobe University Malac, Marek; NRC Harada, Ken; RIKEN Akashi, Tetsuya; Hitachi Ltd Ohmido, Nobuko; Kobe University, Graduate School of Human Development and Environment Fukui, Kiichi; Osaka University, Graduate School of Pharmaceutical Sciences
Keywords:	Chromosomes, TEM, Electron diffraction, Electron Tomography
Keywords:	FIB/SEM, 3D structure, Higher-order structure, Chromatin fibres
Abstract:	It is well known that two DNA molecules are wrapped around histone octamers and folded together to form a single chromosome. However, the nucleosome fiber folding within a chromosome remains an enigma and the higher-order structure of chromosomes also is not understood. In this study, we employed electron diffraction (ED) which provides a non-invasive analysis to characterize the internal structure of chromosomes. The results revealed the presence of structures with 125 to 150 nm periodic features directionally perpendicular to the chromosome axis in unlabelled isolated human chromosomes. We also visualized the 100 to 200 nm periodic features perpendicular to the chromosome axis in an isolated chromosome whose DNA molecules were

	specifically labelled with OsO ₄ using electron tomography (ET) in 300 kV and 1 MeV transmission electron microscopes.

SCHOLARONE™
Manuscripts

1 The higher-order structure of human chromosomes observed by electron diffraction and electron
2 tomography

3 Misa Hayashida^{1*++}, Rinyaporn Phengchat²⁺⁺, Marek Malac^{1,6}, Ken Harada³, Tetsuya Akashi⁴, Nobuko
4 Ohmido², Kiichi Fukui^{5*}

5 ¹ NRC-NANO, National Research Council, 11421 Saskatchewan Drive, T6G 2M9, Edmonton, Alberta,
6 Canada

7 ² Graduate School of Human Development and Environment, Kobe University, 3-11 Tsurukabuto, Nada-
8 ku, 657-8501, Kobe, Japan

9 ³ Center for Emergent Matter Science (CEMS), RIKEN, Hatoyama, Saitama 350-0395, Japan

10 ⁴ Research & Development Group, HITACHI, Ltd., Hatoyama, Saitama 350-0395, Japan

11 ⁵ Graduate School of Pharmaceutical Sciences, Osaka University, 1-6 Yamadaoka, Suita 565-0871,
12 Osaka, Japan

13 ⁶ Department of Physics, University of Alberta, Edmonton, T6G 2E1, Canada

14 ++ Equally contributed

15 *Corresponding authors

16

17 **Abstract**

18 It is well known that two DNA molecules are wrapped around histone octamers and folded together to
19 form a single chromosome. However, the nucleosome fiber folding within a chromosome remains an
20 enigma and the higher-order structure of chromosomes also is not understood. In this study, we employed
21 electron diffraction (ED) which provides a non-invasive analysis to characterize the internal structure of
22 chromosomes. The results revealed the presence of structures with 125 to 150 nm periodic features
23 directionally perpendicular to the chromosome axis in unlabelled isolated human chromosomes. We also
24 visualized the 100 to 200 nm periodic features perpendicular to the chromosome axis in an isolated
25 chromosome whose DNA molecules were specifically labelled with OsO₄ using electron tomography
26 (ET) in 300 kV and 1 MeV transmission electron microscopes.

27 **1. Introduction**

28 The higher-order structure of chromosomes—i.e. their internal structure on a length scale of tens to
29 hundreds of nanometers—has been an enigma for over a century. Several models have been proposed to
30 explain how a chromosome is organized (Beseda et al., 2020; Fukui & Uchiyama, 2007; Ushiki et al.,
31 2002). Models of chromosome higher-order structure are based on the same fundamental premise of DNA
32 wrapping around histones to form nucleosomes. Nucleosomes are connected by links of DNA forming a
33 ‘beads-on-a-string’ structure, referred to as an 11-nm chromatin fiber based on the 11-nm diameter of
34 nucleosomes. From this starting point, the proposed models differ in how the 11-nm chromatin fibers are

35 folded into a chromosome. The hierarchical folded-fiber models describe the formation of chromatin
36 fibers at a length scale beyond 11-nm, including 30-nm and 100-200-nm chromatin fibers. The formation
37 of a 30-nm chromatin structure is reported repeatedly using reconstituted chromatin (Robinson et al.,
38 2006; Schalch et al., 2005; Song et al., 2014) and chromatin extracted from human cells (Cano et al.,
39 2006; Hancock, 2012; Zhou et al., 2019). The 30-nm chromatin fiber has been detected using various
40 visualizing techniques including scanning electron microscopy (SEM) (Inaga et al., 2007; Taniguchi &
41 Takayama, 1986; Wanner et al., 2005), transmission electron microscopy (TEM) (Maeshima & Eltsov,
42 2008; Maeshima et al., 2005; Marsden & Laemmli, 1979) and TEM tomography (Harauz et al., 1987).
43 Additionally, the 30-nm chromatin fibers are found *in situ* in some organisms, for example in avian
44 erythrocyte and in the sperm of starfish and sea cucumbers (Woodcock, 1994). Larger chromatin
45 structures (100-700 nm) consisting of 30-nm fibers have also been reported (Ohnuki, 1968; Taniguchi &
46 Takayama, 1986; Ushiki et al., 2002), although they have been disputed by other results (Joti et al., 2012).
47 On the contrary, recent study using polymer modeling shows that if the chromatin fibers are organized
48 following the hierarchical model, they will be overly restricted and cannot reproduce the chromatin
49 interaction as obtained from Hi-C analysis. Therefore, an alternative model describing that the mitotic
50 chromosome consists of arrays of consecutive chromatin loops, has been proposed (Naumova et al.,
51 2013). The chromatin loops are arranged disorderly way, having diameters between 5 to 25 nm (Ou et al.,
52 2017; Wako et al., 2020). The higher-order chromatin structures including 30-nm chromatin fibers were
53 not detected in mitotic chromosomes by cryo-EM (Eltsov et al., 2008; Maeshima et al., 2010) and small-
54 angle X-ray scattering (SAXS) (Nishino et al., 2012). The reason for the inconsistencies might arise from
55 artifacts caused by the sample preparation. Chromosome dehydration is considered to be one of the
56 sources of artifacts (Kaneyoshi et al., 2015; Maeshima & Eltsov, 2008). To eliminate dehydration related
57 artifacts, we treated the chromosomes isolated from HeLa cells with ionic liquid, according to the study
58 by Dwiranti et al. (Dwiranti et al., 2012). Ionic liquids are known to coat the exterior and penetrate the
59 interior of the chromosomes, and they are compatible with vacuum conditions in an electron microscope
60 (Ishigaki et al., 2011; Kuwabata et al., 2006; Tsuda et al., 2011; Welton, 1999).

61 Electron diffraction (ED) is frequently used for studying periodicity and orientation of periodic structures
62 of an object. Electron beams offer the advantage of focusing to a small probe. Small-angle x-ray
63 scattering (SAXS), a family of x-ray scattering techniques, has been utilized to investigate the presence
64 of 30-nm chromatin fibers in the past (Chicano et al., 2019; Dwiranti et al., 2012; Nishino et al., 2012).
65 However, forming a small probe with x-rays is difficult. SAXS typically collects average data from
66 thousands of chromosomes suspended in a liquid at random orientations relative to the incident x-ray
67 beam and the x-ray detector. Unlike SAXS, information from an individual chromosome can be acquired
68 by ED in a TEM, because an electron beam can be focused on a small area of the sample (much less than
69 1 μm with a small beam convergence angle that is needed to study large periodicities of the chromosome
70 sample). In addition, it is possible to switch the operating mode of a TEM between the image mode (real
71 space) to the diffraction mode (reciprocal space). Obtaining both ED and an image from *exactly the same*
72 *area* of a chromosome and placing the electron probe onto the precise region of the individual
73 chromosome is critical to understanding the relationship between the chromosome axis direction which is
74 vertical direction of chromosomes and the direction of the periodic features observed in the ED patterns.

75 Electron tomography (ET) in a transmission electron microscope (TEM) enables visualization of the
76 structure of an object in three dimension (3D) at high spatial resolution. Using a dual beam— i.e. a

77 focused ion beam (FIB) instrument with an SEM column—an individual chromosome can be located and
78 placed onto a 360° rotation ET sample holder then observed over a full tilt range ($\pm 90^\circ$) (Tanigaki et al.,
79 2015; Tsuneta et al., 2014). The full tilt range ET allows us to overcome the loss of structural information
80 due to the missing wedge of data and enables us to obtain reconstruction of the chromosome that has
81 isotropic resolution in 3D. Typical chromosome thickness (700 nm or so) is larger than optimum for a
82 medium energy (300 keV) microscope, and this leads to an inelastic background in the images. ED is less
83 sensitive than imaging to sample thickness and is capable of detecting periodic features throughout the
84 thickness of the sample (Jiang et al., 2010).

85 Therefore, we observed structures in unstained chromosomes using ED. Structures with 125 to 150 nm
86 periodic features perpendicular to the chromosome axis were observed in an unlabelled individual
87 chromosome observed by ED with a very high camera length. Additionally, we observed individual
88 metaphase chromosomes labelled with OsO₄ from HeLa cells using the ET in both 300 keV and 1 MeV
89 transmission electron microscopes. The use of 1 MeV of energy allows for the investigation of samples
90 with a greater thickness than that allowed by the 300 keV microscope. In the same way as for the ED
91 results, a chromosome extracted from a TEM grid using a dual beam instrument and placed onto a 360°
92 continuous rotation holder (Tanigaki et al., 2015; Tsuneta et al., 2014; Yaguchi et al., 2008) also had 100
93 to 200 nm periodic features perpendicular to a chromosome axis. The ED and ET ability to detect
94 periodicity of structure *internal* to an object, as opposed to on its surface, is an important advantage of ED
95 and ET over scanning electron microscopy (SEM) (Taniguchi & Takayama, 1986) and atomic force
96 microscopy (AFM) (Ushiki et al., 2002) of chromosomes.

97

98

99 2. Materials and Methods

100 2.1 Sample preparation

101 To prepare labelled chromosomes for ET, human chromosomes were isolated from HeLa cells and stored
102 in a polyamine buffer solution (PA chromosomes) as described in Hayashihara et al. (Hayashihara et al.,
103 2008). The buffer solution containing the chromosomes was then dropped onto Carbon/Fomvar support
104 film on a TEM grid on ice and fixed with 2.5% glutaraldehyde for 1 hour. Chromosomes were labelled
105 using ChromEM, a DNA-labeling method developed for electron microscope observation (Ou et al.,
106 2017). After the glutaraldehyde fixation, chromosomes on the TEM grid were labelled with DRAQ5
107 (Abcam), a DNA-specific fluorescence dye. The grid was then transferred into a glass bottom dish
108 containing 2.5 mM diaminobenzidine (DAB, Sigma) in ice-cold 0.1 M sodium cacodylate buffer. The
109 dish was placed under a fluorescence microscope (BX60, Olympus) and chromosomes were fluorescence
110 illuminated continuously with a Cy5 filter set for 20-30 min using a 40x objective lens. Polymerized DAB
111 precipitated on chromosomes made the chromosomes appear brownish. After DAB polymerization, the
112 chromosomes were rinsed with a 0.1M sodium cacodylate buffer and labelled with 2% osmium tetroxide
113 (OsO₄, Electron Microscopy Sciences) in 0.15 M sodium cacodylate for 30 min. The chromosomes were
114 washed with milli-Q water before being treated with 0.5% BMI-BF₄ (ionic liquid, (Dwiranti et al., 2012;
115 Welton, 1999)) in milli-Q water for 1 min at room temperature. Excess ionic liquid solution was removed
116 from the Carbon/Fomvar support film by blotting with cut filter paper, followed by drying in a desiccator
117 equipped with a vacuum pump for 2 hours. For ET, a chromosome was transferred from the
118 Carbon/Fomvar support film and transferred to a 360° rotation holder in a focused ion beam instrument
119 using the method described in our previous paper (Phengchat et al., 2019). Nano dot markers (Hayashida

120 et al., 2014) were fabricated on the carbon support film near the chromosome for the alignment of
121 tomography tilt series images.

122 For the preparation of unlabelled chromosomes for ED, human chromosomes were isolated from HeLa
123 cells and dropped onto Carbon/Fomvar support film on a TEM grid on ice. The samples were then fixed
124 with 2.5% glutaraldehyde for 1 hour on ice. After the washing of glutaraldehyde, the unlabeled
125 chromosomes were directly treated with 0.5% ionic liquid (BMI-BF₄), followed by drying in a vacuum
126 desiccator for 2 hours. ED of the chromosomes was observed directly on the Carbon/Fomvar support film
127 without a transfer onto the 360° rotation tomography holder.

128 2.2 Electron diffraction

129 ED measurements were performed in a Hitachi HF-3300 TEM operated at 300 kV acceleration voltage.
130 The diffraction patterns were collected from unlabelled chromosomes using a Gatan Ultrascan 1000™
131 slow scan CCD camera binned by a factor of 2 to 1024 x 1024 pixels. The diffraction camera length of
132 $L=23.4$ m was obtained by adjusting the projector lens current in a free-lens control mode of the
133 microscope. The large camera length, together with the high brightness cold field emission source of the
134 Hitachi HF-3300, is needed to detect the presence of features with tens to hundreds of nanometers of
135 periodicity, i.e. to study spatial frequencies from ~ 0.1 to less than 0.01 nm^{-1} . In a typical set-up for ED,
136 such large features are buried in the tails of the un-scattered electron beam because the diffraction camera
137 length L is normally less than 3 m. The electron beam was focused into a 750-nm diameter probe placed
138 within a chromosome to prevent diffraction features arising from the edge of a chromosome. The rotation
139 angle between features in a diffraction pattern and the corresponding image that arises due to the use of
140 magnetic lenses in the free lens mode of the TEM was calibrated using a multi-wall carbon nanotube
141 sample. All diffraction patterns reported in this paper were compensated for the rotation angle between
142 the image and the corresponding diffraction pattern.

143

144 2.3 Electron tomography

145 Electron tomography requires the acquisition of a tilt series of TEM images. Typically, low contrast
146 biological samples are stained by a heavy metal (e.g. OsO₄). The heavy metal staining can lead to a
147 sample mass thickness that is too large for a medium (e.g. 300 keV) incident electron energy. To ensure
148 that the features we observed were not artifacts of multiple scattering in a sample with large mass
149 thickness, we observed the samples in microscopes operating at 300 keV and 1 MeV. At 1 MeV, the
150 observable sample thickness increased as compared to that at 300 keV because of the increase in the
151 elastic and inelastic mean free path. We also kept the OsO₄ concentration low to keep the sample mass
152 thickness acceptable for imaging at 300 kV.

153 A Hitachi HF-3300 TEM was operated at 300 kV acceleration voltage. A continuous 360° rotation holder
154 (Yaguchi et al., 2008) was used to collect a tomographic tilt series of the chromosome images stained
155 with OsO₄. Sufficient contrast was obtained in TEM images to observe 100-200 nm periodic structure
156 although the chromosome was rather thick for a 300 keV TEM. The presence of the features was
157 confirmed in a Hitachi 1 MeV TEM (Kawasaki et al., 2000a; Kawasaki et al., 2000b), also equipped with

158 a continuous 360° rotation TEM tomography holder (Tanigaki et al., 2015; Tsuneta et al., 2014). A
159 tomography series consisting of 61 images was collected with a 3° tilt step (Hayashida & Malac, 2016;
160 Hayashida et al., 2018) over the entire 0° to 180° tilt range at both microscopes. The pixel number for
161 HF-3300 and 1MeV FE-TEM were 1024 x 1024 pixels with 4.366 nm/pixel in a Gatan Ultrascan 1000™
162 slow scan CCD camera and 3710×3838 pixels with a 1.77 nm pixel size in a Gatan direct exposure K2
163 camera, respectively. The Simultaneous Iterative Reconstruction Technique (SIRT), as implemented in
164 Composer and Visualizer by TEMography.com, was used for reconstruction of all the tilt series and
165 visualization of the tomograms.

166

167 3. Results

168 3.1 Human chromosomes observed by electron diffraction (ED)

169 Isolated human chromosomes were first examined with ED. In order to optimize the interpretable signal,
170 unlabelled chromosomes were used. Mass thickness of a labelled chromosome is large, leading to large
171 fraction of electrons suffering multiple scattering in the sample and difficult interpretation. Images of the
172 unlabelled chromosomes and the corresponding diffraction pattern are shown in Figs. 1a and 1b,
173 respectively. A circle in Fig. 1a represents an area irradiated by an electron beam probe while collecting
174 the ED pattern, and the dotted line was drawn manually along a chromosome axis which is approximately
175 parallel to the long arm of the chromosome. The pixel with the maximum intensity was selected as a
176 center of the diffraction pattern in Fig. 1b. To detect the presence of features with 100 to 300 nm
177 periodicity within a chromosome (Taniguchi & Takayama, 1986; Ushiki et al., 2002), the measured
178 diffraction intensity was integrated over a scattering angle range from 0.0033 to 0.1 nm⁻¹ at each
179 azimuthal angle α as shown in Fig. 1c. The maximum peak in such spatial frequency-integrated
180 diffraction was detected using an in-house developed Matlab™ code. In this case, the strongest peak
181 appeared at 144°, as shown in Fig 1c. A line profile along the dashed lines $\alpha=144^\circ$ in Fig. 1b is shown in
182 Fig. 1d. A broad peak shown in Fig. 1d indicates that there are features with an approximately 125 nm
183 period at $\alpha=144^\circ$, i.e. in a direction nearly parallel to the chromosome axis ($\alpha=152^\circ$). The dashed line in
184 the diagram on the right top corner in Fig. 1d represents the direction at $\alpha=144^\circ$, and the solid lines show
185 the 125 nm periodic features which are perpendicular to the dashed line. The circle is the same size as the
186 beam area in Fig. 1a. It means that in the beam area in Fig. 1a, there would be fewer than 6 periods of the
187 125 nm features within the electron beam probe. Similar periodic features, with 150 and 133 nm
188 periodicity, were also observed in other chromosomes as shown in Figs. S1 and S2.

189 The diffraction data indicates that the 125 nm periodic features are directionally oriented because they
190 appear only at a particular direction. If the 125 nm periodic features were perfectly oriented against the
191 Carbon/Formvar film, we could see peaks at both 144° and 324° (=144° +180°). However, since the
192 sample is somewhat tilted relative to the incident electron beam, there may be considerable excitation
193 error (Reimer & Kohl, 2008), and therefore we cannot detect the diffraction peak at 324°. Unlike in
194 material science crystalline samples such as silicon and gold thin films, it is difficult to compensate for
195 the excitation error in an experiment on chromosomes due to the poor visibility caused of the weak
196 diffraction pattern features. As a result, only one of the two (complex conjugate) features was observed in
197 our current results (Reimer & Kohl, 2008).

198

199 3.2 Human chromosomes observed by electron tomography (ET)

200 **Isolated human chromosomes whose DNA molecules were labelled with OsO₄ were observed with ET**
201 **using 300keV TEM.** Figs. 2a and 2b show a TEM image and the contrast adjusted image of the
202 chromosome. Periodic features with 100 to 200 nm were observed in the long arm. Fig. 2c and 2d- are Z
203 slice images from the reconstructed tomogram. The slices are closer to both the top and bottom surfaces
204 (Carbon/Formvar film). While the periodic features are visible in Fig 2c, there are no clearly observable
205 features in Fig 2d. When isolated chromosomes are placed on the film, their bottom sides become
206 flattened to maximize their contact with the support film to reduce surface energy (Hayashida et al.,
207 2015). As a result, the bottom side of each chromosome was flatter than their top surface that was not in a
208 contact with a film. As a result, the periodic features were not visible at the bottom side of chromosomes
209 that is in contact with the support film. **Presumably, the features would be observable on both the top and**
210 **the bottom for a chromosome in liquid vitrified by High pressure freezing (McDonald & Auer, 2006)**
211 **although we have to be careful if the procedure changes chromosome structures.**

212 Fig. 3a shows a tomogram of another isolated human chromosome observed with ET using 1 MeV TEM.
213 The chromosome was transferred from the same TEM grid as the chromosome shown in Fig. 2a. Both the
214 upper and lower images in Fig. 3b were extracted from Fig. 3a, and their contrast was enhanced. Periodic
215 features with 100 to 200 nm were also observed as marked by red lines in the lower image in Fig. 3b.

216

217 4. Discussion

218 In this study, we utilized the advantages of electron diffraction (ED) and electron tomography (ET) to
219 examine how nucleosome fibers are organized inside a single chromosome. In unlabeled chromosomes,
220 the diffraction intensity peaks corresponding to more than 125 nm periodic feature (e.g. 133 nm and 150
221 nm) were detected from several isolated chromosomes. **Similar periodic features were also observable in**
222 **OsO₄-DNA labelled chromosomes in TEMs with 300 kV and 1 MV acceleration voltages.** We refer to the
223 more than 100 nm and less than 200 nm periodic features as “Structure A”.

224 Although we did not detect a visible contrast of Structure A in TEM images of unlabelled chromosomes
225 in Fig. 1a, S1a and S2a, all ED patterns show a peak between 100-200 nm. It suggests that the peaks of
226 ED patterns were generated by the density change due to presence of Structure A within the
227 chromosomes. Moreover, the results show that presence of Structure A is not an artifact due to staining as
228 the samples were unstained.

229 Structure A could possibly correspond to the gyres (a repeating structure on DT40 chromosomes-DAPI
230 stained) as reported (Gibcus et al., 2018), and the gyres of coils in spiralized chromosomes reported
231 (Ohnuki, 1968). The gyres visualized in chromosome arms corresponded to the helical arrangement of
232 chromatin loop arrays emanating from a central spiral-staircase (condensin) scaffold (Gibcus et al., 2018).
233 The polymer simulation model predicted that the pitch of the (condensin) scaffold helix could be
234 increased from 100 nm to 200 nm upon prolonged colcemid treatment. We observed Structure A in ED
235 and ET and it oriented nearly perpendicular to the chromosome axis. Therefore, we consider that these

236 features could correspond to the chromatin loop arrays. However, we hypothesized that the condensation
237 status of observed chromosomes (our isolated chromosomes were in a hypercondensed state of 16 h
238 colcemid treatment compared to 1-2.5 h colcemid treatment in previous studies) together with the fixation
239 method between glutaraldehyde and the acid-based fixative could be a reason for the visualization of
240 obvious ~200 nm periodic features. Chromatin loop arrays in each turn of the scaffold helix in our
241 chromosome samples could be tightly packed so that we were unable to observe discrete gyres or
242 spiralized chromosomes. Structure A that we found in this study coincides with the presence of a helical
243 scaffold with ~200 nm pitch in our previous report (Phengchat et al., 2019). By considering the scaffold
244 structure (Phengchat et al., 2019) and the results reported here, both structures of the scaffold and
245 chromatin fibers appear to present the same ~200 nm periodic structure. This suggests that Structure A is
246 a stack of chromatin loop arrays in each turn of the helical chromosome scaffold. It would be worth
247 continuing to develop techniques to simultaneously visualize how nucleosome fibers interact with the
248 chromosome scaffold inside the chromosome.

249 Previous study had observed a fairly homogenous distribution of chromatin fibers inside a human
250 metaphase chromosome using an electron micrograph (Harauz et al., 1987). The chromosomes were
251 prepared from spreads of metaphase lymphocytes on a water surface and absorbed onto TEM grids. The
252 unfixed chromosomes proceeded to ethanol dehydration and critical point drying and were directly
253 observed in TEM without metal staining. The electron micrograph of chromatids clearly showed tangled
254 chromatin fibers that were 30-35 nm in size (Harauz et al., 1987). On the other hand, our ET result
255 showed chromosomes with 100-200 nm of repeated features along the chromatid length. These features
256 were arranged almost perpendicular to the chromosome axis. **The slice image (Fig. 2d) appears uniform
257 with no obvious internal structure. At this point, we hypothesize that the fiber-like features are tightly
258 packed, resulting in extremely low variation in sample mass thickness that in turn makes it impossible for
259 the interface between the fiber-like features to be detected.** Compared with fibrous chromosome structure
260 as reported in Harauz et al. (Harauz et al., 1987), a factor contributing to the different results would be the
261 sample preparation, including fixation, dehydration and staining. Aldehyde-based fixatives performed
262 significantly better in preserving the cellular structure than did organic solvents (Hobro & Smith, 2017).
263 As the chromosome is mainly composed of proteins, glutaraldehyde fixation cross-linking between amino
264 acid groups should be able to keep it intact. **Dehydration and critical point drying in the previous study
265 might introduce cavities into the chromosome, allowing individual ca. 30-35 nm chromatin fibers to be
266 visible. Chen et al. (Chen et al., 2017) provided the information of human prophase chromosome structure
267 through the observation of resin-embedded B lymphocytes with serial block-face scanning electron
268 microscopy (SBF-SEM). Despite the presence cavities found inside the chromosomes, chromosomes
269 were densely packed with more than 90% of chromosome volume was occupied by chromosomal protein-
270 DNA complex (Chen et al., 2017).** In addition, when applied to the unfixed chromosome sample, the
271 dehydration and drying could possibly caused the chromosome structure to shrink and collapse, so that
272 the chromosome could be observed even in 100 kV TEM. **Besides the difference in fixative and
273 dehydration, the DAB polymer specifically deposited on DNA in the chromosome was bound by heavy
274 metal OsO₄, through OsO₄ intensification. This procedure specifically enhances the contrast of chromatin
275 fibers to be observed in TEM.** On the other hand, the contrast from the unstained chromosomes in the
276 previous report (Borland et al., 1988) was due to the structure of both nucleosome fibers and other
277 chromosomal proteins. **The contrast in the entire chromosomes was obvious increased in ChromEM-
278 stained chromosomes, compared to chromosomes with only OsO₄ staining (Fig. S3).**

279 Small-angle X-ray scattering (SAXS) and ultra-SAXS (USAXS) analysis were employed to determine the
280 existence of periodic structures inside the chromosome (Chicano et al., 2019; Nishino et al., 2012). Data
281 obtained from both techniques, supporting cryo-EM observations, suggests that human mitotic
282 chromosomes are composed of irregularly folded nucleosome fibers, rather than 30-nm chromatin fibers
283 or regular structures in the range of 50-1000 nm (Chicano et al., 2019; Nishino et al., 2012). In this study,
284 ED was used to detect any periodic structures inside a single chromosome which the orientation of the
285 chromosome toward the incident electron beam could be managed. Thus, we ensured the presence of
286 Structure A being 150-200 nm in size in each chromosome. The peaks from Structure A were not as sharp
287 as those from metal crystal samples because there are only 5-6 periods in the beam irradiated areas and
288 each piece is not the exact same size. However, the peaks were observed only from the specific direction
289 which is nearly parallel to the chromosome axis — that is, the structures are nearly perpendicular to the
290 chromosome axis.

291 Combining results obtained from ED and ET, it appears that chromatin loop arrays emanating from the
292 central chromosome scaffold are gathered into stacks with the height comparable to the pitch of the
293 helical scaffold (100-200 nm).

294

295 5. Conclusion

296 We found that there are 100 to 200 nm periodic features, “Structure A” perpendicular to a chromosome
297 axis of OsO₄ labelled samples by ET. Structures with 125 to 150 nm periodic features perpendicular to the
298 chromosome axis were also observed in an unlabelled isolated chromosome observed by ED. The
299 structure of the scaffold with similar periodicity was also observed in our previous paper (Phengchat et
300 al., 2019). It therefore emphasizes the essential role of chromosome scaffold in the mitotic chromosome
301 formation. This result might be related to other results (Chicano et al., 2019; Daban, 2015; Gibcus et al.,
302 2018) which showed the fibers or plains along a chromosome axis. We will continue to study both
303 structures of DNA fibers and scaffold to solve the enduring enigma of the chromosome structure.

304

305

306 Acknowledgements

307 This work was supported by the Japan Society for the Promotion of Science (JSPS) KAKENHI
308 (A25252064, 2012 to 2016) and the Japan Science and Technology Agency (JST) SICORP (17935614,
309 2017 to 2022) to Kiichi Fukui and The Mitsubishi Foundation: 202010011 to Nobuko Ohmido.

310

311

312 Figure captions

313 Figure 1 (a) A TEM image of the unlabelled chromosome. The circle represents an area irradiated by an
314 electron beam for ED. (b) An ED pattern from (a). (c) Sum of intensity between 0.0033 and 0.1 and nm^{-1}
315 at each angle: α . (d) Line profile along the line at $\alpha=144^\circ$ in (a).

316 Figure 2 (a) A TEM image of a chromosome labelled with OsO_4 . (b) Contrast enhanced image of (a). (c)
317 and (d) Z slice images from the tomogram of the chromosome. (c) is closer to the top surface of the
318 chromosome and (d) is closer to the bottom surface (Formvar/Carbon film).

319 Figure 3 (a) A tomogram of a chromosome labelled with OsO_4 . (b) Contrast enhanced images extracted
320 from (a). Both images are the same. Lines were drawn in the lower image.

321

322 Figure S1

323 (a) A TEM image of the unlabelled chromosome. The circle represents an area irradiated by an electron
324 beam for ED. (b) Line profile along the line at $\alpha=262^\circ$ from the diffraction pattern from the circle area in
325 (a).

326

327 Figure S2

328 (a) A TEM image of the unlabelled chromosome. The circle represents an area irradiated by an electron
329 beam for ED. (b) Line profile along the line at $\alpha=336^\circ$ from the diffraction pattern from the circle area in
330 (a).

331 **Fig. S3 ChromEM staining in isolated chromosomes (a) Isolated chromosomes either with or without**
332 **DRAQ5 staining were visualized under optical microscope (40X objective lens) before and after photo-**
333 **oxidation. Scale bar = 5 μm (b) Isolate chromosomes visualized with transmitted light under optical**
334 **microscope (100X objective lens) after OsO_4 intensification. Scale bar = 2 μm**

335

336 References

- 337 Beseda, T., Cápál, P., Kubalová, I., Schubert, V., Doležel, J. & Šimková, H. (2020). Mitotic chromosome
338 organization: General rules meet species-specific variability. *Comput. Struct. Biotechnol. J.*
339 Borland, L., Harauz, G., Bahr, G. & Heel, M.v. (1988). Packing of the 30 nm chromatin fiber in the human
340 metaphase chromosome. *Chromosoma* **97**, 159-163.
341 Cano, S., Caravaca, J.M., Martin, M. & Daban, J.R. (2006). Highly compact folding of chromatin induced
342 by cellular cation concentrations. Evidence from atomic force microscopy studies in aqueous
343 solution. *Eur Biophys J* **35**(6), 495-501.
344 Chen, B., Yusuf, M., T. Hashimoto, Estandarte, A., Thompson, G. & Robinson, I. (2017). Three-
345 dimensional positioning and structure of chromosomes in a human prophase nucleus. *Sci. Adv.*
346 **3**, e1602231.
347 Chicano, A., Crosas, E., Oton, J., Melero, R., Engel, B.D. & Daban, J.R. (2019). Frozen-hydrated chromatin
348 from metaphase chromosomes has an interdigitated multilayer structure. *EMBO J* **38**(7).

- 349 Daban, J.R. (2015). Stacked thin layers of metaphase chromatin explain the geometry of chromosome
350 rearrangements and banding. *Sci Rep* **5**, 14891.
- 351 Dwiranti, A., Lin, L., Mochizuki, E., Kuwabata, S., Takaoka, A., Uchiyama, S. & Fukui, K. (2012).
352 Chromosome observation by scanning electron microscopy using ionic liquid. *Microsc. Res.*
353 *Tech.* **75**(8), 1113-1118.
- 354 Eltsov, M., MacLellan, K.M., Maeshima, K., Frangakis, A.S. & Dubochet, J. (2008). Analysis of cryo-
355 electron microscopy images does not support the existence of 30-nm chromatin fibers in mitotic
356 chromosomes in situ. *PNAS* **105**, 19732–19737.
- 357 Fukui, K. & Uchiyama, S. (2007). Chromosome Protein Framework from Proteome Analysis of Isolated
358 Human Metaphase Chromosomes. *Chem. Rec.* **7**, 230-237.
- 359 Gibcus, J.H., Samejima, K., Goloborodko, A., Samejima, I., Naumova, N., Nuebler, J., Kanemaki, M.T., Xie,
360 L., Paulson, J.R., Earnshaw, W.C., Mirny, L.A. & Dekker, J. (2018). A pathway for mitotic
361 chromosome formation. *Science* **359**(6376).
- 362 Hancock, R. (2012). Structure of metaphase chromosomes: a role for effects of macromolecular
363 crowding. *PLoS One* **7**(4), e36045.
- 364 Harauz, G., Borland, L., Bahr, G.F., Zeitler, E. & Heel, M.v. (1987). Three-dimensional reconstruction of a
365 human metaphase chromosome from electron micrographs. *Chromosoma* **95**, 366-374.
- 366 Hayashida, M., Kumagai, K. & Malac, M. (2015). Three dimensional accurate morphology measurements
367 of polystyrene standard particles on silicon substrate by electron tomography. *Micron* **79**, 53-58.
- 368 Hayashida, M. & Malac, M. (2016). Practical electron tomography guide: Recent progress and future
369 opportunities. *Micron* **91**, 49-74.
- 370 Hayashida, M., Malac, M., Bergen, M. & Li, P. (2014). Nano-dot markers for electron tomography formed
371 by electron beam-induced deposition: nanoparticle agglomerates application. *Ultramicroscopy*
372 **144**, 50-57.
- 373 Hayashida, M., Ogawa, S. & Malac, M. (2018). Evaluation of electron tomography reconstruction
374 methods for interface roughness measurement. *Microscopy Research Technique* **81**(5), 515-519.
- 375 Hayashihara, K., Uchiyama, S., Kobayashi, S., Yanagisawa, M., Matsunaga, S. & Fukui, K. (2008). Isolation
376 method for human metaphase chromosomes. *Protoc. Exch.*, 166.
- 377 Hobro, A.J. & Smith, N.I. (2017). An evaluation of fixation methods: Spatial and compositional cellular
378 changes observed by Raman imaging. *Vib. Spectrosc.* **91**, 31-45.
- 379 Inaga, S., Tanaka, K. & Ushik, T. (2007). *Transmission and scanning electron microscopy of mammalian*
380 *metaphase chromosomes*. In: Fukui, K and Ushiki T eds. FL, USA: Boca Raton: CRC Press.
- 381 Ishigaki, Y., Nakamura, Y., Takehara, T., Nemoto, N., Kurihara, T., Koga, H., Nakagawa, H., Takegami, T.,
382 Tomosugi, N., Miyazawa, S. & Kuwabata, S. (2011). Ionic liquid enables simple and rapid sample
383 preparation of human culturing cells for scanning electron microscope analysis. *Microsc Res*
384 *Tech* **74**(5), 415-420.
- 385 Jiang, H., Chen, J. & Malac, M. (2010). Study of the Rhodium Nanoparticles in ZrO₂-CeO₂ Based Catalytic
386 Materials using Nano Beam Diffraction and High Resolution TEM. *Microsc. Microanal.* **16**, 1514-
387 1515.
- 388 Joti, Y., Hikima, T., Nishino, Y., Kamada, F., Hihara, S., Takata, H., Ishikawa, T. & Maeshima, K. (2012).
389 Chromosomes without a 30-nm chromatin fiber. *Nucleus* **3**(5), 404-410.
- 390 Kaneyoshi, K., Fukuda, S., Dwiranti, A., Kato, J., Otsuka, Y., Takata, H., Uchiyama, S., Ogawa, S. & Fukui, K.
391 (2015). Effects of dehydration and drying steps on human chromosome interior revealed by
392 focused ion beam/scanning electron microscopy (FIB/SEM). *Chromosome Sci.* **18**, 23–28.
- 393 Kawasaki, T., Matsui, I., Yoshida, T., Katsuta, T., Hayashi, S., Onai, T., Furutsu, T., Myochin, K., Numata,
394 M., Mogaki, H., Gorai, M., Akashi, T., Kamimura, O., Matsuda, T., Osakabe, N., Tonomura, A. &

- 395 Kitazawa, K. (2000a). Development of a 1 MV field-emission transmission electron microscope. *J.*
396 *Electron Microsc.* **6**, 711-718.
- 397 Kawasaki, T., Yoshida, T., Matsuda, T., Osakabe, N. & Tonomura, A. (2000b). Fine crystal lattice fringes
398 observed using a transmission electron microscope with 1 MeV coherent electron waves. *Appl.*
399 *Phys. Lett.* **76**, 1342-1344.
- 400 Kuwabata, S., Kongkanand, A., Oyamatsu, D. & Torimoto, T. (2006). Observation of Ionic Liquid by
401 Scanning Electron Microscope. *Chem. Lett.* **35**(6), 600-601.
- 402 Maeshima, K. & Eltsov, M. (2008). Packaging the genome: the structure of mitotic chromosomes. *J*
403 *Biochem* **143**(2), 145-153.
- 404 Maeshima, K., Eltsov, M. & Laemmli, U.K. (2005). Chromosome structure: improved immunolabeling for
405 electron microscopy. *Chromosoma* **114**(5), 365-375.
- 406 Maeshima, K., Hihara, S. & Eltsov, M. (2010). Chromatin structure: does the 30-nm fibre exist in vivo?
407 *Curr Opin Cell Biol* **22**(3), 291-297.
- 408 Marsden, M.P. & Laemmli, U.K. (1979). Metaphase chromosome structure: Evidence for a radial loop
409 model. *Cell* **17**, 849-858.
- 410 McDonald, K.L. & Auer, M. (2006). High-Pressure Freezing, Cellular Tomography, and Structural Cell
411 Biology. *BioTechniques* **137**, 137-143.
- 412 Naumova, N., Imakaev, M., Fudenberg, G., Zhan, Y., Lajoie, B.R., Mirny, L.A. & Dekker, J. (2013).
413 Organization of the Mitotic Chromosome. *Science* **342**, 948-953.
- 414 Nishino, Y., Eltsov, M., Joti, Y., Ito, K., Takata, H., Takahashi, Y., Hihara, S., Frangakis, A.S., Imamoto, N.,
415 Ishikawa, T. & Maeshima, K. (2012). Human mitotic chromosomes consist predominantly of
416 irregularly folded nucleosome fibres without a 30-nm chromatin structure. *EMBO J* **31**(7), 1644-
417 1653.
- 418 Ohnuki, Y. (1968). Structure of chromosomes I. Morphological studies of the spiral structure of human
419 somatic chromosomes. *Chromosoma* (25), 402-428.
- 420 Ou, H.D., Phan, S., Deerinck, T.J., Thor, A., Ellisman, M.H. & O'Shea, C.C. (2017). ChromEMT: Visualizing
421 3D chromatin structure and compaction in interphase and mitotic cells. *Science* **357**(6349).
- 422 Phengchat, R., Hayashida, M., Ohmido, N., Homeniuk, D. & Fukui, K. (2019). 3D observation of
423 chromosome scaffold structure using a 360 degrees electron tomography sample holder. *Micron*
424 **126**, 102736.
- 425 Reimer, L. & Kohl, H. (2008). *Transmission Electron Microscopy*. Springer-Verlag New York.
- 426 Robinson, P.J.J., Fairall, L., T, H.V.A. & Rhodes, D. (2006). EM measurements define the dimensions of
427 the "30-nm" chromatin fiber Evidence for a compact, interdigitated structure. *PNAS* **103**(17),
428 6506-6511.
- 429 Schalch, T., Duda, S., Sargent, D.F. & Richmond, T.J. (2005). X-ray structure of a tetranucleosome and its
430 implications for the chromatin fibre. *Nature* **436**(7047), 138-141.
- 431 Song, F., Chen, P., Sun, D., Wang, M., Dong, L., Liang, D., Xu, R.-M., Zhu, P. & Li, G. (2014). Cryo-EM Study
432 of the Chromatin Fiber Reveals a Double Helix Twisted by Tetranucleosomal Units. *Science* **344**,
433 376-380.
- 434 Tanigaki, T., Takahashi, Y., Shimakura, T., Akashi, T., Tsuneta, R., Sugawara, A. & Shindo, D. (2015).
435 Three-dimensional observation of magnetic vortex cores in stacked ferromagnetic discs. *Nano*
436 *Lett* **15**(2), 1309-1314.
- 437 Taniguchi, T. & Takayama, S. (1986). High-order structure of rectaphase chromosomes: Evidence for a
438 multiple coiling model. *Chromosoma* **93**, 511-514.
- 439 Tsuda, T., Nemoto, N., Kawakami, K., Mochizuki, E., Kishida, S., Tajiri, T., Kushibiki, T. & Kuwabata, S.
440 (2011). SEM observation of wet biological specimens pretreated with room-temperature ionic
441 liquid. *Chembiochem* **12**(17), 2547-2550.

- 442 Tsuneta, R., Kashima, H., Iwane, T., Harada, K. & Koguchi, M. (2014). Dual-axis 360 degrees rotation
443 specimen holder for analysis of three-dimensional magnetic structures. *Microscopy* **63**(6), 469-
444 473.
- 445 Ushiki, T., Hoshi, O., Iwai, K.I., Kimura, E. & Shigeno, M. (2002). The structure of human metaphase
446 chromosomes: its histological perspective and new horizons by atomic force microscopy. *Arch.*
447 *Histol. Cytol.* **65**(5), 377-390.
- 448 Wako, T., Yoshida, A., Kato, J., Otsuka, Y., Ogawa, S., Kaneyoshi, K., Takata, H. & Fukui, K. (2020). Human
449 metaphase chromosome consists of randomly arranged chromatin fibres with up to 30-nm
450 diameter. *Sci Rep* **10**(1), 8948.
- 451 Wanner, G., Schroeder-Reiter, E. & Formanek, H. (2005). 3D analysis of chromosome architecture:
452 advantages and limitations with SEM. *Cytogenet Genome Res* **109**(1-3), 70-78.
- 453 Welton, T. (1999). Room-Temperature Ionic Liquids. Solvents for Synthesis and Catalysis. *Chem. Rev.* **99**,
454 2071-2083.
- 455 Woodcock, C.L. (1994). Chromatin Fibers Observed In Situ in Frozen Hydrated Sections. Native Fiber
456 Diameter Is Not Correlated with Nucleosome Repeat Length. *J. Cell Biol.* **125**(1), 11-19.
- 457 Yaguchi, T., Konno, M., Kamino, T. & Watanabe, M. (2008). Observation of three-dimensional elemental
458 distributions of a Si device using a 360 degrees -tilt FIB and the cold field-emission STEM system.
459 *Ultramicroscopy* **108**(12), 1603-1615.
- 460 Zhou, Z., Li, K., Yan, R., Yu, G., Gilpin, C.J., Jiang, W. & Irudayaraj, J.M.K. (2019). The transition structure
461 of chromatin fibers at the nanoscale probed by cryogenic electron tomography. *Nanoscale* **11**,
462 13783 - 13789.

463

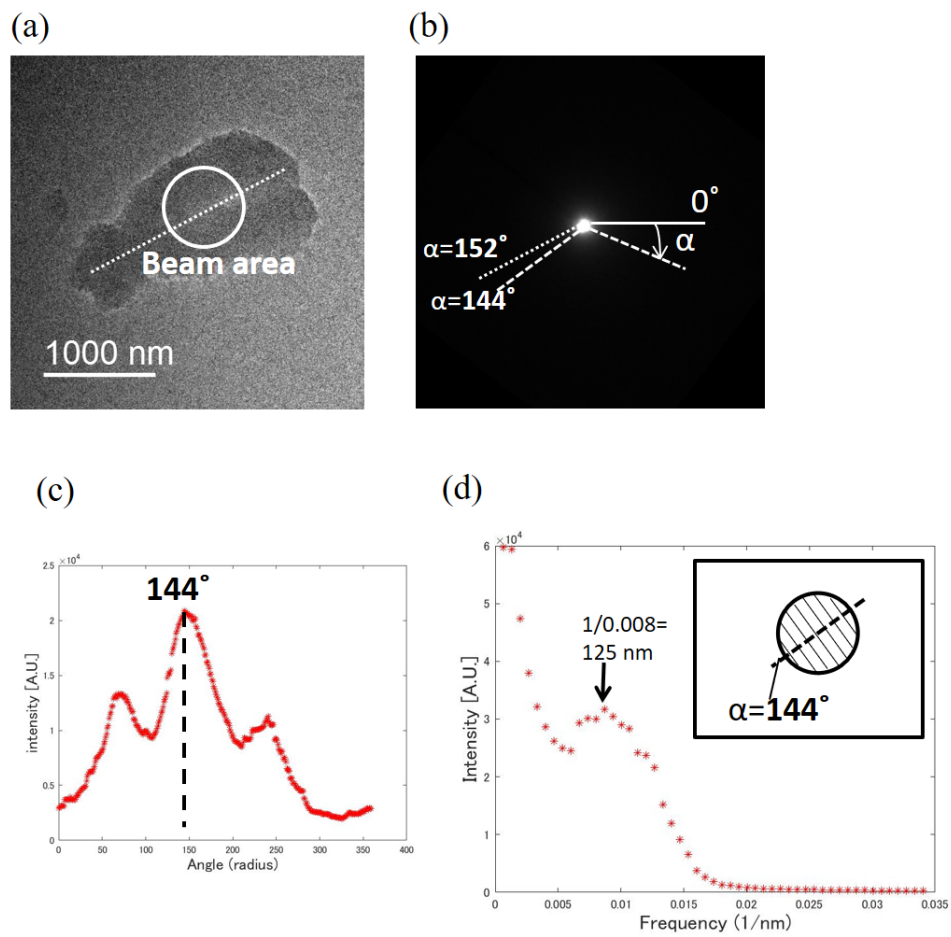


Figure 1 (a) A TEM image of the unlabelled chromosome. The circle represents an area irradiated by an electron beam for ED. (b) An ED pattern from (a). (c) Sum of intensity between 0.0033 and 0.1 and nm^{-1} at each angle: α . (d) Line profile along the line at $\alpha = 144^\circ$ in (a).

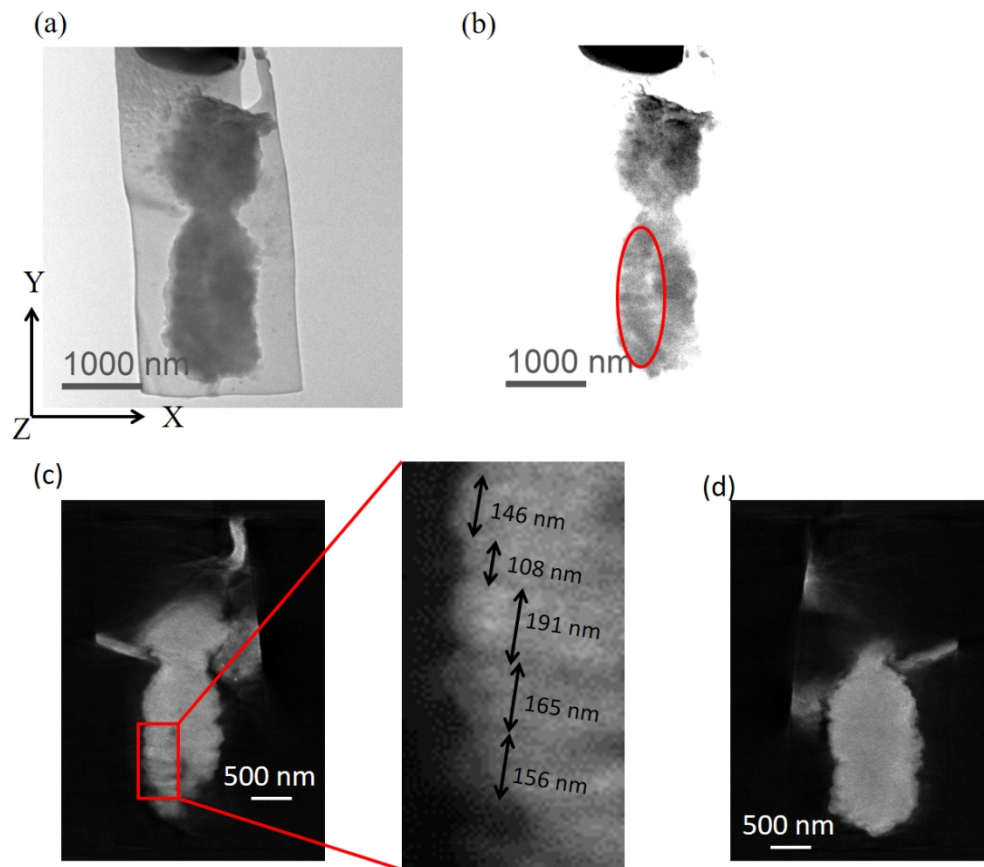


Figure 2 (a) A TEM image of a chromosome labelled with OsO₄. (b) Contrast enhanced image of (a). (c) and (d) Z slice images from the tomogram of the chromosome. (c) is closer to the top surface of the chromosome and (d) is closer to the bottom surface (Formvar/Carbon film).

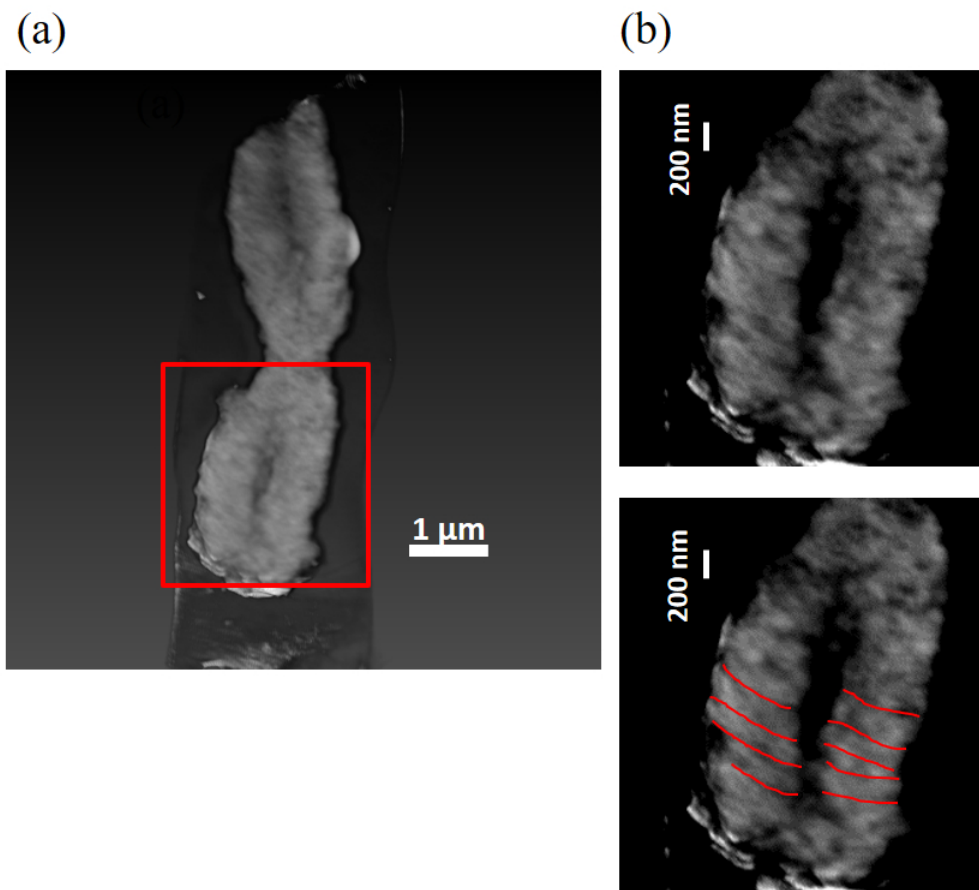


Figure 3 (a) A tomogram of a chromosome labelled with OsO₄. (b) Contrast enhanced images extracted from (a). Both images are the same. Lines were drawn in the lower image.

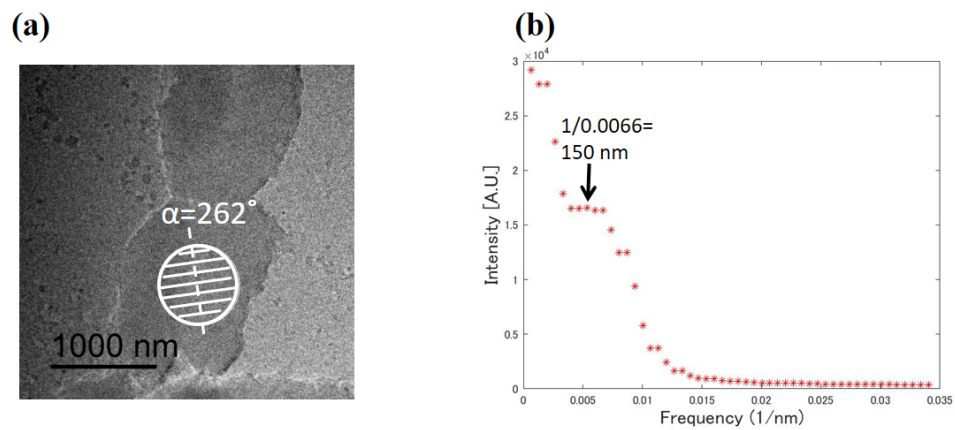


Figure S1 (a) A TEM image of the unlabelled chromosome. The circle represents an area irradiated by an electron beam for ED. (b) Line profile along the line at $\alpha = 262^\circ$ from the diffraction pattern from the circle area in (a).

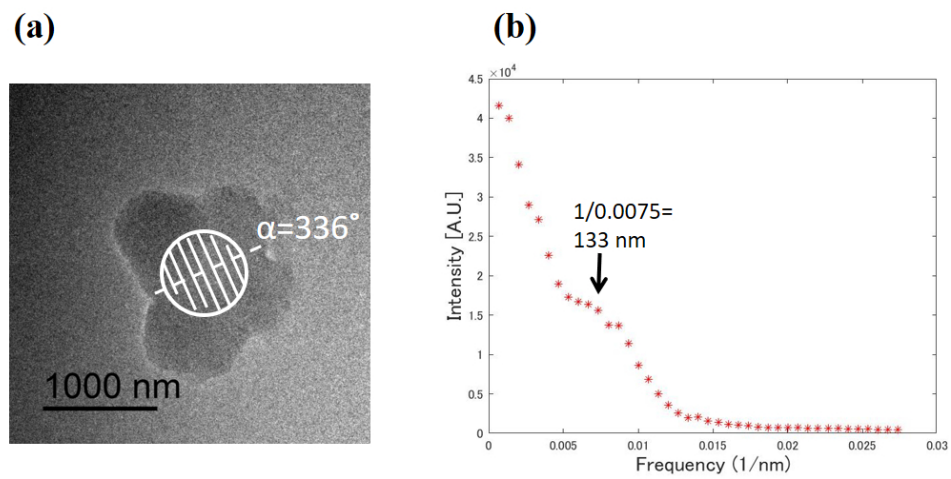


Figure S2 (a) A TEM image of the unlabelled chromosome. The circle represents an area irradiated by an electron beam for ED. (b) Line profile along the line at $\alpha = 336^\circ$ from the diffraction pattern from the circle area in (a).

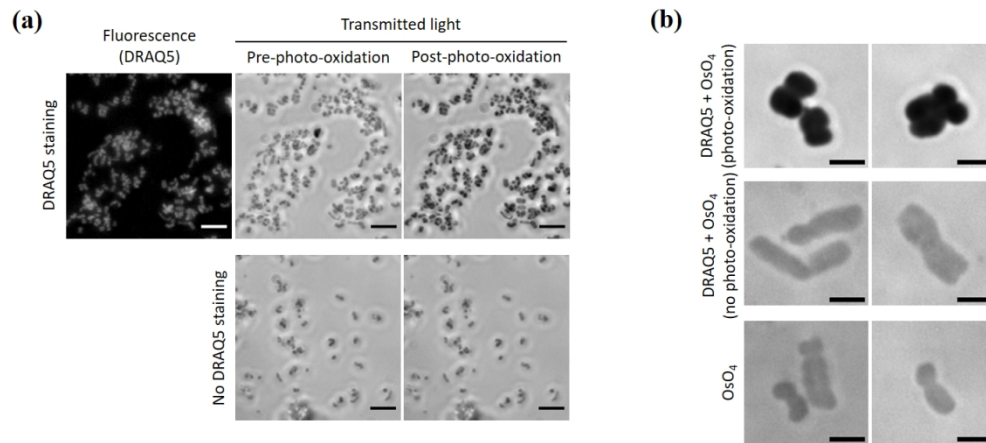


Fig. S3 ChromEM staining in isolated chromosomes (a) Isolated chromosomes either with or without DRAQ5 staining were visualized under optical microscope (40X objective lens) before and after photo-oxidation. Scale bar = 5 μm (b) Isolate chromosomes visualized with transmitted light under optical microscope (100X objective lens) after OsO_4 intensification. Scale bar = 2 μm